Palaeogeography, Palaeoclimatology, Palaeoecology 441 (2016) 360–376

Contents lists available at ScienceDirect

Palaeogeography, Palaeoclimatology, Palaeoecology

journal homepage: www.elsevier.com/locate/palaeo

Terrestrial isotopic evidence for a Middle-Maastrichtian warming event from the lower Cantwell Formation, Alaska

Susana Salazar-Jaramillo [a,1], Sarah J. Fowell [b], Paul J. McCarthy [c], Jeff A. Benowitz [d], Maciej G. Śliwiński [e], Carla S. Tomsich [f]

[a] University of Alaska Fairbanks, Department of Geosciences, and Geophysical Institute, Fairbanks, AK 99775-0948, United States
[b] University of Alaska Fairbanks, Department of Geosciences, Fairbanks, AK 99775-5780, United States
[c] University of Alaska Fairbanks, Department of Geosciences, and Geophysical Institute, Fairbanks, AK 99775-5780, United States
[d] University of Alaska Fairbanks, Department of Geosciences, and Geophysical Institute, Fairbanks, AK 99775-5940, United States
[e] University of Wisconsin-Madison, Department of Geosciences, Madison, WI 53706, United States
[f] University of Alaska Fairbanks, Department of Geosciences, and Geophysical Institute, Fairbanks, AK 99775-5780, United States

ARTICLE INFO

Article history:
Received 21 December 2014
Received in revised form 18 September 2015
Accepted 21 September 2015
Available online 3 October 2015

Keywords:
Lower Cantwell Formation
Zircon U–Pb Geochronology
Carbon Isotope Stratigraphy
Late Cretaceous
Paleoclimate
Middle Maastrichtian Event

ABSTRACT

Carbon stable isotope data ($\delta^{13}C$) and new radiometric dates indicate that the non-marine Late Cretaceous lower Cantwell Formation, central Alaska, registers the Middle-Maastrichtian Event (MME), a global warming episode. A stratigraphic section measured at the East Fork of the Toklat River in Denali National Park & Preserve includes a bentonite layer that we have dated to 69.5 ± 0.7 Ma using U–Pb isotope analysis of zircons. The new depositional age confirms that dinosaur tracks from the lower Cantwell Formation are coeval with dinosaur bones from outcrops of the Prince Creek Formation on Alaska's North Slope. $\delta^{13}C$ data from fossil wood recovered from the lower Cantwell Formation records an ~3‰ positive excursion correlative with positive excursions from terrestrial and marine sections in West Texas (USA) and Gubbio (Italy), respectively. The similarity between marine and terrestrial records suggests that this excursion is the result of a major perturbation in the global carbon cycle, known as the Middle-Maastrichtian Event (MME). Mean annual precipitation (MAP) estimates calculated from $\delta^{13}C$ data yield a range of 168–470 mm/yr during the MME, 353–1050 mm/yr before and 475–1451 mm/yr after the warming event. The $\delta^{13}C$ record from the lower Cantwell Formation provides the first terrestrial high-latitude evidence for the MME, while MAP estimates for the coeval Prince Creek Formation suggest that the arctic coast may have been more humid than southern interior Alaska during the Middle Maastrichtian.

1. Introduction

During the Late Cretaceous a long-term global cooling trend (Li and Keller, 1999) was interrupted at ~69 Ma by an intense greenhouse episode known from terrestrial records as the Middle Maastrichtian Event (MME; Nordt et al., 2003; Dworkin et al., 2005). The MME marks the end of the early Maastrichtian and lasted <1 Ma (Bralower et al., 2002). It is characterized by rapid, 2–3 °C warming of deep and surface ocean waters (Keller, 2001; Bralower et al., 2002; Frank et al., 2005) and terrestrial mean annual temperatures between 21 and 23 °C at a paleolatitude of ~35° N (Nordt et al., 2003). In the marine record, the overall magnitude of the carbon isotope ($\delta^{13}C$) fluctuation is 0.6‰ to 1.5‰, and two positive excursions are separated by a negative inflection (Voigt et al., 2012). In pedogenic carbonate from West Texas, the MME is also defined by two positive peaks separated by a negative inflection of up to 1‰ (Nordt et al., 2003).

The lower Cantwell Formation (Fig. 1) contains abundant plant remains and ichnofossils (Fiorillo et al., 2009a; Fiorillo et al., 2009b; Tomsich et al., 2010; Fiorillo and Adams, 2012; Fiorillo and Tykoski, 2014), allowing reconstruction of fauna and flora that serve as proxies for terrestrial paleoclimatic conditions on a Middle Maastrichtian greenhouse Earth (Spicer and Herman, 2010; Suarez et al., 2013a). In this paper, we describe a high-resolution sedimentary record from the lower Cantwell Formation exposed along the East Fork of the Toklat River, Denali National Park & Preserve, Alaska. A new bentonite U–Pb zircon age of 69.5 ± 0.7 Ma constrains the age of an ~3‰ positive $\delta^{13}C$ excursion recorded by fossil wood and allows chemostratigraphic correlation with other terrestrial and marine $\delta^{13}C$ records of the MME.

Previous studies indicate close coupling of marine, atmospheric, and terrestrial carbon pools during the Cretaceous (Hasegawa, 1997; Gröcke et al., 1999; Gröcke, 2002; Hasegawa et al., 2003; Gröcke et al., 2006; Li et al., 2013; Suarez et al., 2013b; Ludvigson et al., 2015). The similarity between our most significant positive $\delta^{13}C$ excursion and terrestrial

E-mail addresses: ssalazar2@alaska.edu (S. Salazar-Jaramillo), sjfowell@alaska.edu (S.J. Fowell), pjmccarthy@alaska.edu (P.J. McCarthy), jbenowitz@alaska.edu (J.A. Benowitz), msliwinski@wisc.edu (M.G. Śliwiński), cstomsich@alaska.edu (C.S. Tomsich).
[1] Present address: Department of Geosciences, National University of Colombia, Bogotá, Colombia. Tel.: +51 3165000.

http://dx.doi.org/10.1016/j.palaeo.2015.09.044
0031-0182/

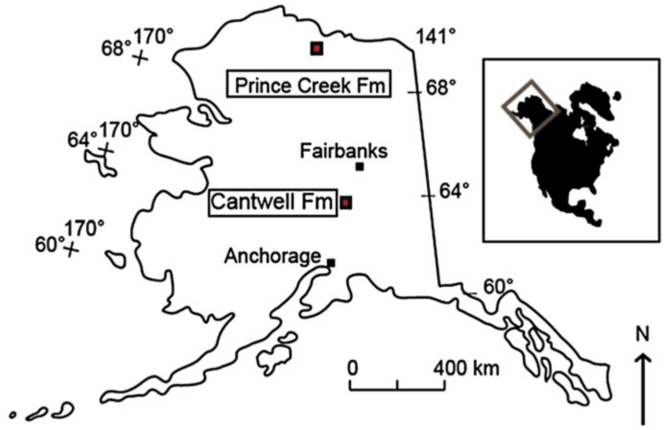

Fig. 1. Map of Alaska showing approximate locations of the Cantwell Formation and the coeval Prince Creek Formation.

and marine carbonate excursions from coeval sites in West Texas (USA) and Gubbio (Italy) suggests that the MME was a major perturbation in the global carbon cycle.

2. Geologic setting

Southern Alaska is the product of collisional events that added juvenile crust to western North America (Trop and Ridgway, 2007). The Cantwell Basin (Fig. 1) developed in the vicinity of the suture zone following Mesozoic accretion of the Wrangellia composite terrane to the North American Cordilleran margin (Ridgway et al., 1997; Trop and Ridgway, 2007). Continued northward thrusting of the Kahiltna assemblage and the Wrangellia composite terrane against the Yukon–Tanana terrane during the Campanian–Maastrichtian resulted in development of the Cantwell thrust-top basin. This two-sided basin is characterized by alluvial, fluvial, lacustrine and minor marine depositional systems (Ridgway et al., 1997; Tomsich et al., 2014). Highlands to the south were created by syndepositional displacement on south-dipping thrust faults, while the north side of the basin was filled by sediment derived from erosion of uplifted, quartz-rich metamorphic rocks of the Yukon–Tanan terrane (Trop and Ridgway, 2007). Dominance of nonmarine deposition and petrographic evidence for sediment derived from both oceanic and continental source rocks indicate that deposition of the lower Cantwell Formation and regional subaerial uplift of the suture zone between the Yukon–Tanana and Wrangellia composite terranes were coeval (Ridgway et al., 2002). The Cantwell Basin was at an approximate paleolatitude of 71 ± 10° N (Hillhouse and Coe, 1994) during deposition of the upper Cantwell Formation.

The Cantwell Formation is currently bounded to the south by the Denali fault and to the north by the Hines Creek fault, both part of a major strike-slip fault system (Ridgway et al., 1997, Nokleberg et al., 2013). It is subdivided into two lithologic units, a lower sedimentary unit and an upper volcanic unit (Ridgway et al., 1997; Trop and Ridgway, 2007), herein termed lower and upper Cantwell Formation, respectively. The two units are separated by an angular unconformity that represents a hiatus of approximately 10–20 Ma (Cole et al., 1999). The lower Cantwell Formation is a Late Cretaceous (Campanian–Maastrichtian) heterogeneous non-marine to marginal marine succession composed of conglomerate, sandstone, siltstone, shale, coaly shale, minor coal and oncolitic limestone, mudstone, local paleosols, and altered tuffs (Wolfe and Wahrhaftig, 1970; Ridgway et al., 1997; Ridgway et al., 2002; Tomsich et al., 2014). Sediment is interpreted to have been deposited primarily in stream-dominated alluvial fans, axial braided streams, and lacustrine environments (Ridgway et al., 1997; Tomsich et al., 2014). The upper Cantwell Formation is a volcanic unit of Paleocene–Eocene age which consists of basalt, minor basaltic andesite, rhyolite, pyroclastic flows and minor volcaniclastic rocks, with the oldest volcanic rocks dating to 59.8 ± 0.2 Ma ($^{40}Ar/^{39}Ar$ whole rock; Cole et al., 1999).

The age of the lower Cantwell Formation has been a subject of some debate due to conflicting results from paleofloristic analyses (Wolfe and Wahrhaftig, 1970) and K–Ar radiometric age determinations (Sherwood and Craddock, 1979) on intrusive granite stocks. Subsequent palynological analyses indicate that the lower Cantwell Formation was deposited during the late Campanian and early Maastrichtian (Ridgway et al., 1997). Recent work dating bentonite layers within the lower Cantwell Formation has provided additional age constraints. Tomsich et al. (2014) employed U–Pb geochronology to date two bentonite samples collected from outcrops of the lower Cantwell Formation near Sable Mountain, Denali National Park & Preserve, to ~71.5 +/− 0.9 Ma and 71.0 +/− 1.1 Ma, respectively.

3. Methods

3.1. Sedimentology

Stratigraphic sections of the lower Cantwell Formation that crop out along the East Fork of the Toklat River were measured with a Jacob Staff. The S-2 section, 122.45 m thick, was selected for detailed facies and stable isotopic analyses because it contains abundant leaf impressions, wood, dinosaur tracks, pedogenic features (burrows, root traces, and redoximorphic features), and a single bentonite layer. The facies analysis (Tables 1 and 2) was carried out using a facies classification modified from Miall (1996).

3.2. Bentonite U–Pb zircon age

Four liters (~2 kg) of a ~10 cm thick white bentonite unit were collected from the S-2 section (Fig. 2). Zircon grains were isolated and prepared at Apatite to Zircon, Inc., using standard mineral separation procedures described by Donelick et al. (2005). The bentonite sample was crushed into 2–3 mm fragments and sieved through a 300 μm nylon mesh. The <300 μm size fraction was washed, and zircons were separated using lithium metatungstate, a Frantz magnetic separator, diodomethane, and hand-panning separation procedures. The zircon separates were mounted in epoxy and polished to expose the grains. Laser ablation-inductively coupled plasma-mass spectrometry (LA-ICP-MS) analysis was performed using a New Wave YP213 213 nm solid state laser ablation system and a Thermo Scientific Element2 magnetic sector mass spectrometer at the Washington State University Geoanalytical Laboratory in Pullman, Washington.

Analytical procedures employed by Apatite to Zircon, Inc. for U–Pb zircon data are based on a model that constrains background-corrected signal intensities measured for each isotope (^{206}Pb, ^{232}Th, and ^{238}U) and the degree of fractionation resultant of radiation damage to the crystal lattice from a total of 250 scans performed at each laser ablation spot on zircon standards and samples during a single sample analysis session. Zircon U–Pb standards with accepted ages ranging from 1099.00 Ma (primary standard) to 28.201 Ma were treated as unknowns to calibrate fractionation factors and absolute errors. Results of each scan were smoothed according to standard procedures, and deviations from the accepted ages for each zircon standard were used to monitor and correct for cumulative radiation damage during sample scans. Concordance was monitored separately for each ablation spot. Decay constants used in the age equation and the $^{238}U/^{235}U$ isotopic ratio are those of Steiger and Yäger, 1977 cited in Chew and Donelick, 2012. $^{207}Pb/^{235}U$, $^{206}Pb/^{238}U$, and $^{207}Pb/^{206}Pb$ ages were calculated for each data scan and checked for concordance; herein concordance is defined as congruence of all three ages at the 1σ level. Typically, if the number of concordant scans for a spot is greater than zero, the more precise age from the concordant-scan-weighted ratios $^{207}Pb/^{235}U$, $^{206}Pb/^{238}U$, or $^{207}Pb/^{206}Pb$ is chosen as the preferred age. Compound error calculations for the isotopic ratios include background-corrected signal values for each isotopic ratio, the